Clin Orthop Relat Res (2008) 466:273–280
DOI 10.1007/s11999-007-0061-y

SYMPOSIUM: PAPERS PRESENTED AT THE ANNUAL CLOSED MEETING OF THE INTERNATIONAL HIP SOCIETY

Hip Damage Occurs at the Zone of Femoroacetabular Impingement

M. Tannast MD, D. Goricki MD, M. Beck MD, S. B. Murphy MD, K. A. Siebenrock MD

Abstract Although current concepts of anterior femoroacetabular impingement predict damage in the labrum and the cartilage, the actual joint damage has not been verified by computer simulation. We retrospectively compared the intraoperative locations of labral and cartilage damage of 40 hips during surgical dislocation for cam or pincer type femoroacetabular impingement (Group I) with the locations of femoroacetabular impingement in 15 additional hips using computer simulation (Group II). We found no difference between the mean locations of the chondrolabral damage of Group I and the computed impingement zone of Group II. The standard deviation was larger for measures of articular damage from Group I in comparison to the computed values of Group II. The most severe hip damage occurred at the zone of highest probability of femoroacetabular impact, typically in the anterosuperior quadrant of the acetabulum for both cam and pincer type femoroacetabular impingements. However, the extent of joint damage along the acetabular rim was larger intraoperatively than that observed on the images of the 3-D joint simulations. We concluded femoroacetabular impingement mechanism contributes to early osteoarthritis including labral lesions.

Level of Evidence: Level II, diagnostic study. See the Guidelines for Authors for a complete description of levels of evidence.

One or more of the authors has received funding from the National Center for Competence in Research "Computer Aided and Image Guided Medical Interventions (Co-Me)" (MT, KAS), a fellowship for prospective researchers of the Swiss National Science Foundation (SNF) (MT), a Travel Fellowship Award from the International Society for Computer Assisted Orthopaedic Surgery (CAOS International) (MT), and the 2005 Research Grant Award from the New England Baptist Hospital (MT, SBM).
Each author certifies that his or her institution has approved the human protocol for this investigation, that all investigations were conducted in conformity with ethical principles of research, and that informed consent for participation in the study was obtained.

M. Tannast (✉), D. Goricki, M. Beck, K. A. Siebenrock
Department of Orthopaedic Surgery, Inselspital, University of Bern, Murtenstrasse 3010 Bern, Switzerland
e-mail: moritz.tannast@insel.ch

S. B. Murphy
Center for Computer Assisted and Reconstructive Surgery, New England Baptist Hospital, Tufts University, Boston, MA, USA

Introduction

Femoroacetabular impingement (FAI) is a recently proposed etiology of early osteoarthritis of the young hip [8, 18]. It represents an abutment conflict between the acetabular rim and the proximal femur of hips that appear "normal" at first sight on conventional radiographs. Osseous prominences of the femur and/or the acetabulum expose the hip to recurrent microtrauma during certain torsional maneuvers of the joint (particularly end-range flexion and internal rotation) leading to degenerative joint alterations. Two types of impingement have been distinguished based on the origin and the mechanism of impingement: pincer and cam [2, 11]. Pincer impingement occurs when there is direct linear contact with an abrupt stop between the femoral head–neck junction and a localized anterior osseous acetabular prominence (eg, with acetabular retroversion) [20] or generally overcovered acetabulum (eg, protrusio acetabuli) [8]. Cam impingement is mainly caused by a femoral head that is not perfectly round which subsequently is jammed into the acetabulum [9].

The typical location of early chondrolabral damage is located in the anterosuperior quadrant of the acetabulum [1, 2, 21]. According to the FAI theory, the articular damage occurs at the site of highest femoroacetabular impact. However, the actual articular damage has not been correlated to known zones of impingement owing to lack of a validated noninvasive method to ascertain impingement during motion. Existing imaging methods only include a "static" interpretation of the joint damage (eg, conventional radiography [24], magnetic resonance imaging [12], or 3-D computed tomography [CT] [1]). Previously described "dynamic" imaging methods for simulating hip range of motion and individual femoroacetabular impingement location [22] have not been validated with actual motion and impingement in cadavers either. In addition, they do not include the software requirements to ascertain cumulative impingement zones, but rather provide a single impingement point and not areas of impingement based on a given range of motion.

We hypothesized the locations of labral and cartilage degeneration occur at the computed zone of FAI for both pincer and cam hips.

Materials and Methods

We retrospectively compared the intraoperatively documented location and extent of degenerative articular joint damage of one group of hips (Group I; n = 40) with the location of impingement detected with specifically developed software from a second independent group of hips (Group II; n = 15). In Group I, the intraoperative joint damage including locations was documented for each patient by the surgeon during the surgical hip dislocation. In Group II, a recently developed computer analysis described later was performed preoperatively. We compared the locations of labral damage and cartilage damage along the acetabular rim for the two groups.

All patients from both groups had been diagnosed with anterior FAI. The diagnosis was based on previously described clinical and radiographic criteria [8, 18, 24]. All patients had a positive "impingement sign" on clinical examination [8]. Two subgroups in both groups I and II were established: a cam subgroup and a pincer subgroup. A hip was classified as spherical if the head protruded out of a circle drawn around the head and extended anteriorly in a convex shape of the base of the neck on the lateral crosstable view [2]. The shape of the femoral head was classified as normal if the femoral head was spherical both in the anteroposterior and the axial crosstable radiograph, the neck offset measured less than 7 mm [6], or the alpha angle according to Nötzli et al. [19] measured less than 50°. The acetabulum was classified as retroverted if the anterior acetabular rim was more lateral than the posterior rim in the cranial part of the acetabulum [20, 24]. A coxa profunda was diagnosed if the floor of the acetabulum touched or overlapped the ilioischial line [2, 3, 24]. A protrusio was identified when the femoral head overlapped the ilioischial line medially [2, 3, 24].

For Group I, we reviewed the intraoperative notes of 263 consecutive patients (302 hips, 39 bilateral) who underwent surgical hip dislocation for FAI at the senior author's (KAS) institution. We included only hips with a pure cam or pincer FAI according to the criteria by Beck et al. [2] because these two groups have substantially different patterns of joint damage. We excluded 109 hips with combined FAI, 52 hips with advanced osteoarthritis (Grade ≥ 1 according to Tönnis [25]), 37 with traumatic or posttraumatic conditions, 36 with insufficient/incomplete radiographs, 14 with avascular necrosis, seven with previous surgery, and seven with Legg–Calvé–Perthes disease, leaving 40 hips (32 patients, 8 bilateral) with pure cam or pincer types for further investigation. We compared demographic, clinical, and radiographic parameters to match study cohorts. There were no differences of the evaluated parameters (Table 1). This project was approved by the local institutional review board.

Intraoperatively, we (MB, KAS, RG, ML) assessed the labrum and the acetabular cartilage. The labrum was judged damaged if there was evidence of a complete tear, tear of the undersurface, or degenerative changes within the substance (Fig. 1A) [2]. The cartilage was judged damaged if there were signs of degeneration ranging from roughening of the surface with fibrillation to full-thickness defects (Fig. 1B) [3]. To describe the exact location of the lesions, the acetabulum was divided into 12 sectors corresponding to a clock face, the 6 o'clock being located in the middle of the incision acetabular notch (Fig. 1C). All findings were converted to the right side to have 3 o'clock consistently representing the most anterior portion of the acetabulum. The lesions of the labrum and cartilage were assigned numbers correlating with their position. Because the identifications of the quality [4, 13] of cartilage and the extent of labrum lesions with the clock system [16] is accurate in other, more complex joints, we did not perform an additional intra/interobserver analysis of these assessments. For this group, no preoperative computer analysis was performed because all patients had been operated before the software had been validated (see "HipMotion," below).

For Group II, we reviewed the digital image database of one of the authors (SBM). In this center, a noninvasive CT-based 3-D impingement analysis is performed routinely for patients with FAI. From a total of 59 hips (51 patients, 8 bilateral) and based on the inclusion/exclusion criteria on anteroposterior (Fig. 2A) and crosstable axial radiographs (Fig. 2B) described above, we identified 15 hips (9

Table 1. Comparison of both study groups

Parameter	Group I	Group II	p Value
Number of hips	40	15	
Bilateral hips (% bilateral)	20%	40%	0.965
Analysis	Intraoperative observation of labrum and cartilage damage	Computer calculation of impingement zones	
Type of impingement			
Cam	24	9	
Pincer	16	6	
Age (years)	33.4 ± 8.8 (17.7–54.6)	35.7 ± 9.7 (20.2–48.8)	0.439
Gender (% male)	65%	80%	0.231
Side (% right)	59%	60%	0.558
Height (cm)	176.2 ± 9.5 (159–196)	176.5 ± 5.7 (165–185)	0.875
Weight (kg)	79.6 ± 15.3 (50–120)	87.4 ± 18.0 (59–127)	0.150
Body mass index (kg/m^2)	25.5 ± 4.2 (18.1–35.4)	27.8 ± 4.6 (21.6–37.1)	0.103
Flexion (degrees)	100.6 ± 13.4 (70–125)	98.7 ± 5.2 (75–105)	0.511
Internal rotation (degrees)	11.3 ± 10.2 (–5–30)	5.8 ± 8.2 (–15–15)	0.080
External rotation (degrees)	29.4 ± 12.8 (0–70)	27.8 ± 3.9 (20–30)	0.941
Adduction (degrees)	22.2 ± 9.1 (10–40)	18.2 ± 6.2 (0–20)	0.284
Abduction (degrees)	30.4 ± 10.8 (5–45)	26.6 ± 4.6 (5–30)	0.120
ACM angle (degrees)			
All hips	44.2 ± 3.0 (39–50)	44.2 ± 4.7 (38–53)	0.922
Cam hips	44.0 ± 3.7 (39–50)	44.8 ± 6.0 (38–53)	0.759
Pincer hips	44.7 ± 2.4 (40–48)	46.0 ± 4.4 (43–51)	0.663
Extrusion index (%)			
All hips	16.4 ± 9.1 (–3–32)	13.3 ± 10.2 (–3–31)	0.283
Cam hips	17.8 ± 9.2 (0–32)	17.2 ± 10.8 (0–31)	0.883
Pincer hips	9.3 ± 6.6 (–3–18)	3.3 ± 6.1 (–3–12)	0.110
Crossover sign (% positive)	53%	65%	0.290
Lateral center edge angle (degrees)			
All hips	35.8 ± 9.2 (20–59.1)	34.6 ± 8.6 (20–58.7)	0.655
Cam hips	29.2 ± 7.8 (20–56)	26.8 ± 9.8 (20–41.2)	0.404
Pincer hips	40.1 ± 11.1 (19–59.1)	40.7 ± 15.3 (25–58.7)	0.985
Posterior wall sign (% positive)	53%	65%	0.290
Retroversion index (%)*	28.1 ± 22.9 (5.4–74.4)	27.6 ± 17.6 (5.3–53.7)	0.947
Centrum collum diaphyseal angle (degrees)	128.8 ± 8.8 (116–148)	126 ± 7.3 (114–138)	0.478
Alpha angle (degrees)			
All hips	74.1 ± 20.1 (30–110)	65.4 ± 16.7 (36–92)	0.127
Cam hips	77.5 ± 18.0 (50–110)	76.6 ± 13.0 (53–92)	0.904
Pincer hips	44.6 ±7.6 (30–49)	42.3 ± 4.2 (36–49)	0.546

Values are expressed as mean ± standard deviation, with range in parentheses; *only in patients with a positive crossover sign.

patients, 6 bilateral) with pure pincer or cam impingement. A virtual 3-D model of the hip and the distal part of the femur was acquired using a standard helical scanner for CT scans. For this group, no comparable intraoperative data were available for two reasons: the surgeon used an alternative less invasive surgical approach without full acetabular visualization (11 hips [7 patients]), or patients refused operation (4 hips [2 patients]).

We used a previously developed and validated software called "HipMotion" (University of Bern, Switzerland) for all hips, allowing anatomically based calculation of the individual hip range of motion, the location of impingement zones, and quantified surgical virtual treatment of FAI surgery (Fig. 2C) [22]. Anatomic references for the calculation of the amplitude of hip motion were the anterior pelvic plane for the pelvis [5, 23] and the axis through

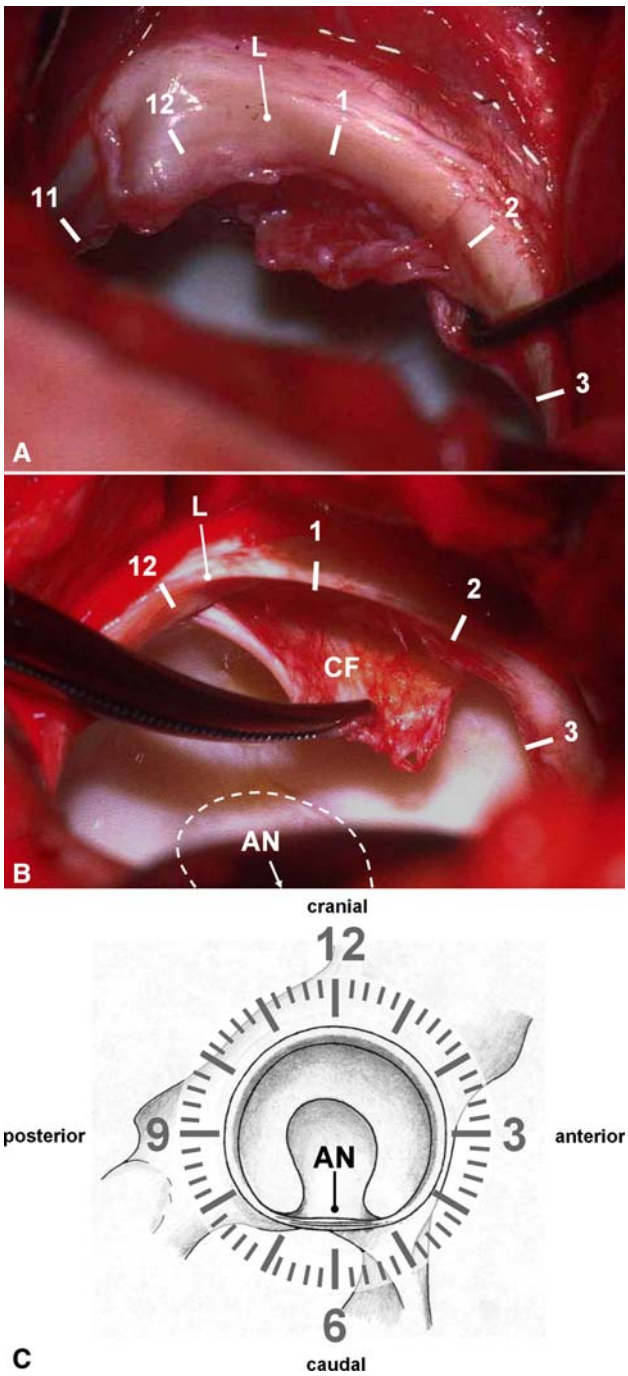

Fig. 1A–C (**A**) A labrum (L) was judged damaged if there was evidence for a complete tear, tear of the undersurface, or degenerative changes within the substance. In this case, an undersurface lesion detected with a hook together with degenerative changes can be observed from 11 to 3 o'clock. (**B**) The cartilage was judged damaged if there were signs of degeneration ranging from roughening of the surface with fibrillation to full-thickness defects. In this case, a cartilage flap (CF) can be seen from 12 to 2 o'clock. (**C**) The labral and chondral lesions and the impingement zones were assigned numbers correlating with their positions on a clock face. The 6 o'clock position is located in the middle of the incision acetabular notch (AN).

the hip and knee center for the femur [17]. Based on the motion pattern of conventional manual examination (impingement test [8, 9]), we evaluated the hips in 5° increments between 70° and 110° of flexion and in 10° increments between –20° to 20° of adduction. Internal rotation was restricted by the individual morphology of the joint. We quantified the position of each single impingement point of every possible combination of patterns detected on the acetabular rim, resulting in approximately 2000 to 4000 computed impingement points per patient (Fig. 2C). The distribution of the zones was automatically calculated and virtually documented using the described clock system according to clinical practice.

We created histograms displaying the frequency of distribution of the zone of impingement and the location of the labral and chondral damage. We compared the mean values of the distribution for every possible combination of each group and subgroup.

Because these numbers represent the maximum available numbers with a complete documentation at the authors' departments, we performed no a priori power analysis. Instead, we carried out a post hoc power analysis for the gathered data described later. At a two-sided level of significance of 5%, a power of 73.4% was found for detection of differences between the labrum damage locations and the computed impingement zones and 65.9% for differences between the cartilage damage locations and the computed impingement zones.

We used the Kolmogorov–Smirnov test to determine normal distributions and nonpaired t tests to analyze normally distributed variables (selected demographic parameters [Table 1], localization of intraoperative cartilage and labrum). The continuous demographic parameters of all groups/subgroups had a normal distribution. We used Mann–Whitney U tests to compare nonpaired data without normal distribution (adduction, abduction, external rotation). Differences in standard deviation between the theoretical impingement zones and the actual joint damage were calculated by means of the F test. We performed Fisher's exact test to assess associations between categorical parameters (selected demographical data, eg, gender). Significance was set at the $p < 0.05$ level.

Results

We observed no differences in the mean values of the locations of the detected labrum lesions of Group I and in Group II (Fig. 3A) and for the pincer (Fig. 3B) and cam (Fig. 3C) subgroups (distributions shown in Table 2; p values shown in Table 3). The individual peak of the

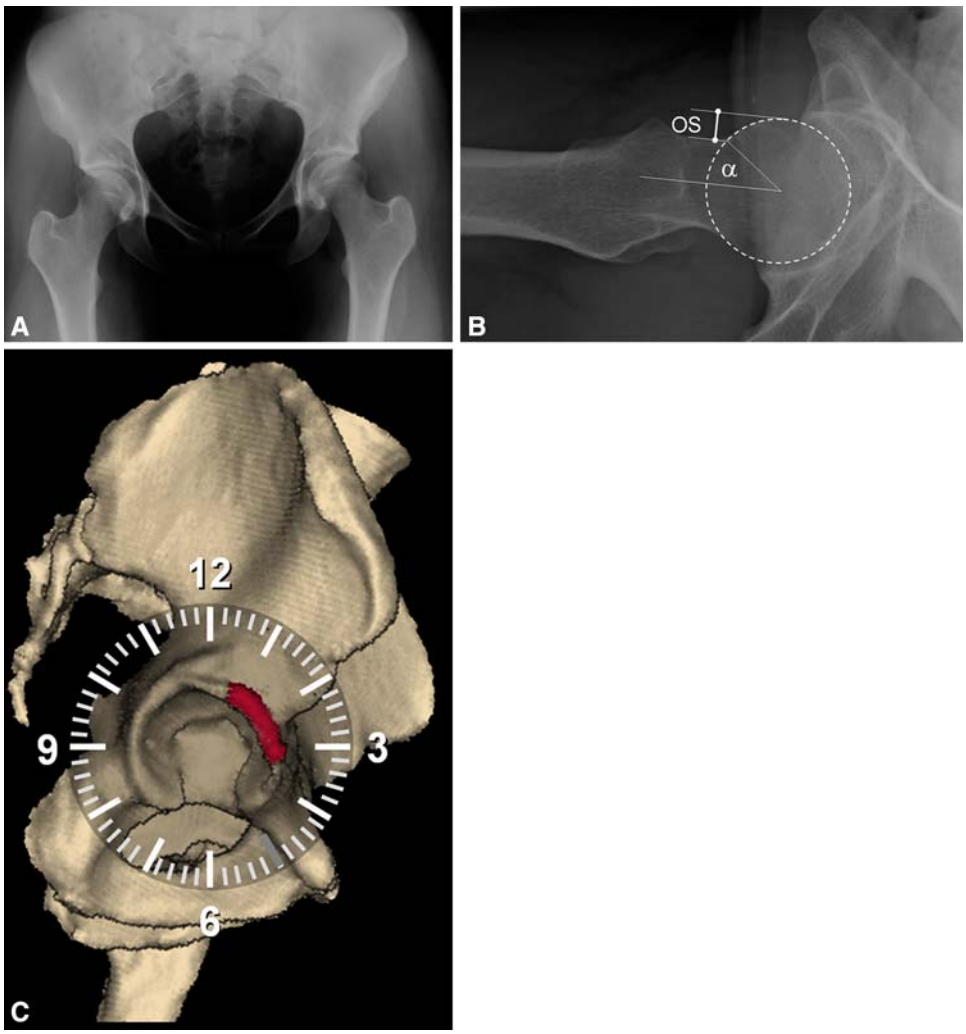

Fig. 2A–C This 26-year-old women presented with symptomatic anterior pincer FAI on the right side. (**A**) The anteroposterior pelvic radiograph reveals a bilateral coxa profunda without acetabular retroversion. (**B**) The femoral head demonstrated no signs of asphericity, the offset (OS) was more than 7 mm, and the alpha angle was 37°. (**C**) This snapshot shows the distribution of the sum of impingement zones for this patient for every possible combination of flexion, internal rotation, and adduction within a predefined maximum range (see text). The zones are located in the anterosuperior quadrant of the acetabulum when evaluating anterior FAI (red area).

normal distribution of the labrum lesions and the computed impingement zones was located in the anterosuperior quadrant of the acetabulum for all subgroups. We found no differences in the mean calculated values of the labrum lesions and impingement zones for cam and pincer hips (Table 3). The comparison of variance of the distribution showed a larger standard deviation of labral lesions when comparing to the computerized impingement zones to both pincer (Fig. 3B) and cam hips (Fig. 3C).

There was no difference in the mean values of the locations of the detected cartilage lesions of Group I and Group II for all three subgroups. (Fig. 3A–C, Tables 2 and 3). The peak of the normal distribution of the cartilage lesions was located in the anterosuperior acetabular quadrant which did not differ from the computed impingement zones for cam or pincer hips (Tables 2 and 3). However, the variance of the distribution was larger for the locations of the chondral lesions compared to those for the computerized impingement zones in both pincer (Fig. 3B) and cam hips (Fig. 3C) (Table 4).

When comparing labral with cartilage lesions, we observed no difference in terms of the mean values of the normal distribution (Table 3). However, we did observe a more circumferential pattern of labral and chondral damage ($p = 0.022$ and $p = 0.05$, respectively) in pincer hips (Table 4).

Discussion

Although the inferential evidence suggests labral and associated early degenerative cartilage damage are related to FAI, the concurrence of the actual impingement zone and resulting joint damage have not been confirmed. We therefore hypothesized the locations of labral and cartilage degeneration occur at the computed zone of impingement for both pincer and cam hips.

We note several limitations. First, we did not correlate the individual damage of one specific patient with the determined impingement in that patient but rather

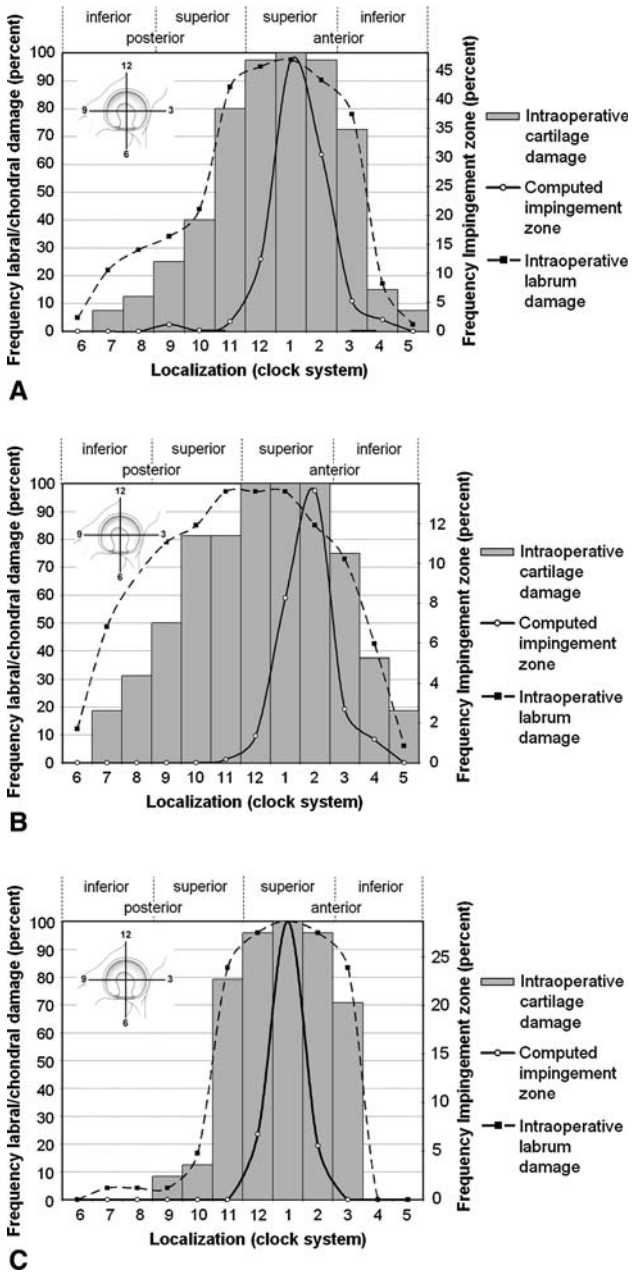

Fig. 3A–C The diagrams show the distribution for both study groups (cartilage and labrum damage separately) in (**A**) all evaluated hips, (**B**) hips with pincer type FAI, and (**C**) hips with cam type FAI. There were no differences in the mean values of the subgroups. However, a substantially larger standard deviation could be found for the labrum and cartilage damage in comparison to the impingement zones for all three subgroups.

correlated locations of observed damage in one group with simulated impingement in another. This relates to several factors. First, not all patients undergoing a CT-based computer analysis of the hip were scheduled for surgery; some of them refused surgery for various reasons (eg, ongoing sports career) or were still deciding whether to have surgery. Second, other patients of Group II

Table 2. Distribution of the detected labral and cartilage lesions and the computed impingement zones along the acetabulum

Group	Subgroup	Location (range, standard deviation)
Group I (labrum)	All	12.1 o'clock (6–5 o'clock, 2.2 hours)
	Cam	12.8 o'clock (7–3 o'clock, 1.6 hours)
	Pincer	12.5 o'clock (6–5 o'clock, 2.7 hours)
Group I (cartilage)	All	12.5 o'clock (7–5 o'clock, 2.0 hours)
	Cam	12.8 o'clock (9–3 o'clock, 1.5 hours)
	Pincer	12.2 o'clock (9–3 o'clock, 1.5 hours)
Group II	All	1.2 o'clock (11–4 o'clock, 1 hour)
	Cam	1.0 o'clock (12–2 o'clock, 0.5 hours)
	Pincer	1.7 o'clock (11–4 o'clock, 0.9 hours)

(particularly patients with cam type FAI) did not undergo a full surgical hip dislocation but had an alternative, less invasive procedure, such as arthroscopy or an anterior approach. Third, some patients already had areas of cartilage loss substantial enough that joint-preserving surgery would likely have failed. However, the demographic, clinical, and radiographic data did not differ between the two groups (Table 1), and the authors believe these two patient populations are comparable. Future studies should include the comparison of the individual femoroacetabular contact zone with the resulting damage within the same patient. Another limitation is the fact that reliability/reproducibility of grading cartilage and labrum lesions and their extension were not specifically investigated in this study. However, previous studies suggest reasonable kappa or intraclass correlation values for these parameters [4, 13, 16]. Marx et al. [13] found an observed agreement of the Outerbridge classification for grading of articular cartilage during knee arthroscopy of 80% to 94% with an overall accuracy of 68%. Similarly, Cameron et al. [4] found an average intraobserver kappa coefficient of 0.80 with an average kappa value of 0.72 for interobserver agreement for grading of chondral lesions in knee arthroscopy. Analogously to the clock system of the hip joint, Mihata et al. [16] evaluated the distribution of labral tears of the shoulder along the glenoid rim and found a mean intraclass correlation coefficient of 0.77 for intraobserver repeatability and 0.72 for interobserver reproducibility. In all these validation studies, the direct intraoperative visualization and palpation of the defects was used as gold standard. Keeping in mind that in our measurements only a binary description system (damaged versus intact) was used and that our data relates to direct intraoperative observation, we do not believe this limitation seriously jeopardizes our data or conclusions even when no comparable data on this subject is available for the hip.

The joint damage we observed along the acetabular rim in anterior FAI was larger than the computed impingement

Table 3. p Values of the t test for comparisons of the mean values of all possible combinations of study groups and subgroups*

Group	Subgroup	Group I (Labrum)			Group I (Cartilage)			Group II		
		All	Cam subgroup	Pincer subgroup	All	Cam subgroup	Pincer subgroup	All	Cam subgroup	Pincer subgroup
Group I (Labrum)	All		0.058	0.761	0.746	0.047	0.029	0.307	0.982	0.418
	Cam	0.058		0.760	0.134	0.091	0.890	0.156	0.484	0.646
	Pincer	0.761	0.760		0.139	0.652	0.489	0.151	0.523	0.728
Group I (Cartilage)	All	0.746	0.134	0.139		0.113	0.081	0.273	0.151	0.138
	Cam	0.047	0.911	0.652	0.113		0.981	0.908	0.464	0.457
	Pincer	0.029	0.890	0.489	0.081	0.981		0.572	0.602	0.583
Group II	All	0.307	0.156	0.147	0.273	0.908	0.572		0.355	0.211
	Cam	0.982	0.484	0.523	0.138	0.464	0.602	0.355		0.678
	Pincer	0.418	0.646	0.728	0.146	0.457	0.583	0.211	0.678	

*All values were normally distributed.

Table 4. p Values of the F test for the comparisons of variances of all possible combinations of study groups and subgroups*

Group	Subgroup	Group I (Labrum)			Group I (Cartilage)			Group II		
		All	Cam subgroup	Pincer subgroup	All	Cam subgroup	Pincer subgroup	All	Cam subgroup	Pincer subgroup
Group I (Labrum)	All		0.292	< 0.01	0.851	0.269	< 0.01	< 0.01	< 0.01	0.098
	Cam	0.292		0.022	0.217	0.957	0.044	< 0.01	< 0.01	< 0.01
	Pincer	< 0.01	0.022		< 0.01	0.025	0.761	< 0.01	< 0.01	< 0.01
Group I (Cartilage)	All	0.851	0.217	< 0.01		0.198	< 0.01	< 0.01	< 0.01	0.140
	Cam	0.269	0.957	0.025	0.198		0.050	< 0.01	< 0.01	0 < 0.01
	Pincer	< 0.01	0.044	0.761	< 0.01	0.050		< 0.01	< 0.01	< 0.01
Group II	All	< 0.01	< 0.01	< 0.01	< 0.01	< 0.01	< 0.01		0.061	< 0.01
	Cam	< 0.01	< 0.01	< 0.01	< 0.01	< 0.01	< 0.01	0.061		0.038
	Pincer	0.098	< 0.01	< 0.01	0.140	< 0.01	< 0.01	< 0.01	0.038	

*All values were normally distributed.

area although the mean values of most frequent impact site and the maximum chondrolabral damage did not differ. Two explanations are conceivable. Our software only calculates the sum of single impingement points of two rigid bodies. The motion simulation stops as soon as an impingement point is detected. It ignores soft tissue and potential bone deformation under stress. It is likely the motion proceeds slightly due to the deformable properties of the cartilage and the labrum, leading to a larger damage of the involved structures. This is supported by the fact that the particular stress distribution of the hip as a ball-and-socket joint is distributed around a maximum pole [27]. The stress distribution therefore is not restricted only to the maximum contact point between the acetabular rim and the femoral head–neck junction but also includes the adjacent chondrolabral structures.

Several theories explain the preponderance of lesions involving the anterior labral–cartilage junction. These include inferior intrinsic mechanical properties compared to other portions of the labrum or a relative hypovascularity making the anterior labrum more vulnerable to wear and degeneration because of resultant compromised remodeling and healing capacity [14, 15]. However, according to our data, it is more likely chondrolabral lesions occur at the site of highest probability of femoroacetabular impact and thus are more exposed to higher mechanical stress.

Our findings support reports in the literature describing an association between the presence of the labral lesions and the degeneration of the adjacent articular surface, mainly proven in arthroscopy [7, 14, 15]. However, all of these studies have in common that they fail to provide a satisfactory explanation for the cause of articular damage. Most authors ascribe direct trauma during sports activities to the etiology of the labral tears. In fact, they rarely occur in the absence of bony abnormalities [26]. The results of arthroscopy with partial limbectomy are therefore

unsatisfactory if the underlying cause (in most cases FAI) is not addressed simultaneously [10]. Based on our analysis and in accordance with other studies [26], we assume, in a substantial number of hips where a labral tear is evident, FAI is the underlying cause.

Our analysis demonstrates the most severe joint damage in anterior FAI occurs directly at the site of highest impact in the anterosuperior quadrant of the labrum. The extent of the resulting degenerative joint alteration along the acetabular rim was larger intraoperatively than that observed on the images of the 3-D joint collision detection. From our data, we concluded (1) the maximum hip damage in FAI occurs at the impingement impact site between the femoral head–neck junction and the acetabulum and (2) an even larger area of damage should be expected intraoperatively compared to a preoperative noninvasive computerized assessment. Based on the evidence, we believe FAI is a major source of early joint damage.

Acknowledgments We thank Dr. Monika Kubiak-Langer, Dr. Frank Langlotz, Rainer Jumpertz, Prof. Reinhold Ganz, and Dr. Michael Leunig for their contributions to this project.

References

1. Beaulé PE, Zaragoza E, Motamedi K, Copelan N, Dorey FJ. Three-dimensional computed tomography of the hip in the assessment of femoroacetabular impingement. *J Orthop Res.* 2005;1286–1292.
2. Beck M, Kalhor M, Leunig M, Ganz R. Hip morphology influences the pattern of damage to the acetabular cartilage: femoroacetabular impingement as a cause of early osteoarthritis of the hip. *J Bone Joint Surg Br.* 2005;87:1012–1018.
3. Beck M, Leunig M, Parvizi J, Boutier V, Wyss D, Ganz R. Anterior femoroacetabular impingement: Part II: Midterm results of surgical treatment. *Clin Orthop Relat Res.* 2004;418:67–73.
4. Cameron ML, Briggs KK, Steadman JR. Reproducibility and reliability of the Outerbridge Classification for grading chondral lesions of the Knee arthroscopically. *Am J Sports Med.* 2003;31:83–86.
5. DiGioia AM, Jaramaz B, Blackwell M, Simon DA, Morgan F, Moody JE, Nikou C, Colgan BD, Aston CA, Labarca RS, Kischell E, Kanade T. The Otto Aufranc Award: Image guided navigation system to measure intraoperatively acetabular implant alignment. *Clin Orthop Relat Res.* 1998;355:8–22.
6. Eijer H, Leunig M, Mahomed MN, Ganz R. Crosstable lateral radiograph for screening of anterior femoral head–neck offset in patients with femoro-acetabular impingement. *Hip Int.* 2001; 11:37–41.
7. Farjo LA, Glick JM, Sampson TG. Hip arthroscopy for acetabular labral tears. *Arthroscopy.* 1999;15:132–137.
8. Ganz R, Parvizi J, Beck M, Leunig M, Nötzli H, Siebenrock KA. Femoroacetabular impingement: a cause for osteoarthritis of the hip. *Clin Orthop Relat Res.* 2003;417:112–120.
9. Ito K, Minka MA 2nd, Leunig M, Werlen S, Ganz R. Femoroacetabular impingement and the cam-effect: a MRI based quantitative anatomical study of the femoral head–neck offset. *J Bone Joint Surg Br.* 2001;83:171–176.
10. Kim KC, Hwang DS, Lee CH, Kwon ST. Influence of femoroacetabular impingement on results of hip arthroscopy in patients with early osteoarthritis. *Clin Orthop Relat Res.* 2007;456: 128–132.
11. Lavigne M, Parvizi J, Beck M, Siebenrock KA, Ganz R, Leunig M. Anterior femoroacetabular impingement: Part I: Techniques of joint preserving surgery. *Clin Orthop Relat Res.* 2004;418: 61–66.
12. Leunig M, Podeszwa D, Beck M, Werlen S, Ganz R. Magnetic resonance arthrography of labral disorders in hips with dysplasia and impingement. *Clin Orthop Relat Res.* 2004;418:74–80.
13. Marx RG, Connor J, Lyman S, Amendola A, Andrish JT, Kaeding C, McCarthy EC, Parker RD, Wright RW, Spindler KP. Multirater agreement of arthroscopic grading of knee articular cartilage. *Am J Sports Med.* 2005;33:1654–1657.
14. McCarthy J, Noble P, Aluisio FV, Schuck M, Wright J, Lee JA. Anatomy, pathologic features, and treatment of acetabular labral tears. *Clin Orthop Relat Res.* 2003;406:38–47.
15. McCarthy JC, Noble PC, Schuck MR, Wright J, Lee J. The Otto E. Aufranc Award: The role of labral lesions to development of early degenerative hip disease. *Clin Orthop Relat Res.* 2001; 393:25–37.
16. Mihata T, McGarry MH, Tibone JE, Abe M, Lee TQ. Type II SLAP lesions: a new scoring system—the sulcus score. *J Shoulder Elbow Surg.* 2005;14(1 Suppl S):19S–23S.
17. Murphy SB, Simon SR, Kijewski PK, Wilkinson RH, Griscom T. Femoral anteversion. *J Bone Joint Surg Am.* 1987;69:1169–1176.
18. Murphy SB, Tannast M, Kim YJ, Buly R, Millis MB. Debridement of the adult hip for femoroacetabular impingement: indications and preliminary clinical results. *Clin Orthop Relat Res.* 2004;429:178–181.
19. Nötzli HP, Wyss TF, Stöcklin CH, Schmid MR, Treiber K, Hodler J. The contour of the femoral head–neck-junction as a predictor for the risk of anterior impingement. *J Bone Joint Surg Br.* 2002;84:556–560.
20. Reynolds D, Lucac J, Klaue K. Retroversion of the acetabulum: a cause of hip pain. *J Bone Joint Surg Br.* 1999;81:281–288.
21. Siebenrock KA, Schöniger R, Ganz R. Anterior femoro-acetabular impingement due to acetabular retroversion and its treatment by periacetabular osteotomy. *J Bone Joint Surg Am.* 2003; 85:278–286.
22. Tannast M, Kubiak-Langer M, Langlotz F, Puls M, Murphy SB, Siebenrock KA. Noninvasive three-dimensional assessment of femoroacetabular impingement. *J Orthop Res.* 2007;25:122–131.
23. Tannast M, Langlotz U, Siebenrock KA, Wiese M, Bernsmann K, Langlotz F. Anatomic referencing of cup orientation in total hip arthroplasty. *Clin Orthop Relat Res.* 2005;436:144–150.
24. Tannast M, Siebenrock KA, Anderson SE. Femoroacetabular impingement: radiographic diagnosis–what the radiologist should know. *AJR Am J Roentgenol.* 2007;188:1540–1552.
25. Tönnis D. General radiography of the hip joint. In: Tönnis D, ed. *Congenital Dysplasia, Dislocation of the Hip*. New York, NY: Springer; 1987:100–142.
26. Wenger DE, Kendell KR, Miner MR, Trousdale RT. Acetabular labral tears rarely occur in the absence of bony abnormalities. *Clin Orthop Relat Res.* 2004;426:145–150.
27. Yoshida H, Faust A, Wilckens J, Kitagawa M, Fetto J, Chao EY. Three-dimensional dynamic hip contact area and pressure distribution during activities of daily living. *J Biomech.* 2006; 39:1996–2004.